



**HAL**  
open science

## **Circulating Cell-Free DNA from Colorectal Cancer Patients May Reveal High KRAS or BRAF Mutation Load**

Florent Mouliere, Safia El Messaoudi, Celine Gongora, Anne-Sophie Guedj, Bruno Robert, Maguy del Rio, Franck Molina, Pierre-Jean Lamy, Evelyne Lopez-Crapez, Muriel Mathonnet, et al.

► **To cite this version:**

Florent Mouliere, Safia El Messaoudi, Celine Gongora, Anne-Sophie Guedj, Bruno Robert, et al.. Circulating Cell-Free DNA from Colorectal Cancer Patients May Reveal High KRAS or BRAF Mutation Load. *Translational Oncology*, 2013, 6 (3), pp.319 - 328. 10.1593/tlo.12445 . hal-01826199

**HAL Id: hal-01826199**

**<https://unilim.hal.science/hal-01826199>**

Submitted on 29 Jun 2018

**HAL** is a multi-disciplinary open access archive for the deposit and dissemination of scientific research documents, whether they are published or not. The documents may come from teaching and research institutions in France or abroad, or from public or private research centers.

L'archive ouverte pluridisciplinaire **HAL**, est destinée au dépôt et à la diffusion de documents scientifiques de niveau recherche, publiés ou non, émanant des établissements d'enseignement et de recherche français ou étrangers, des laboratoires publics ou privés.

## Circulating Cell-Free DNA from Colorectal Cancer Patients May Reveal High *KRAS* or *BRAF* Mutation Load<sup>1,2</sup>

Florent Mouliere<sup>\*,†,‡,§,¶</sup>, Safia El Messaoudi<sup>\*,†,‡,§,¶</sup>,  
Celine Gongora<sup>\*,†,‡,§</sup>, Anne-Sophie Guedj<sup>¶</sup>,  
Bruno Robert<sup>\*,†,‡,§</sup>, Maguy Del Rio<sup>\*,†,‡,§</sup>,  
Franck Molina<sup>¶</sup>, Pierre-Jean Lamy<sup>#</sup>,  
Evelyne Lopez-Crapez<sup>#</sup>, Muriel Mathonnet<sup>\*\*</sup>,  
Marc Ychou<sup>††</sup>, Denis Pezet<sup>‡‡</sup>  
and Alain R. Thierry<sup>\*,†,‡,§,¶</sup>

Institut de Recherche en Cancérologie de Montpellier, Montpellier, France; <sup>†</sup>Institut National de la Santé et de la Recherche Médicale, U896, Montpellier, France; <sup>‡</sup>Université Montpellier 1, Montpellier, France; <sup>§</sup>Institut régional du Cancer Montpellier, Montpellier, France; <sup>¶</sup>Sysdiag UMR3145, Centre National de la Recherche Scientifique/Bio-Rad, Montpellier, France; <sup>#</sup>Laboratoire de Biologie Spécialisée et d'Oncogenetique, Montpellier, France; <sup>\*\*</sup>Centre Hospitalier Universitaire, Service Oncologie Digestive, Limoges, France; <sup>††</sup>Centre Régional de Lutte contre le Cancer Val d'Aurelle-Paul Lamarque, Montpellier, France; <sup>‡‡</sup>Centre Hospitalier Universitaire Estaing, Unité d'Oncologie Digestive, Clermont Ferrand, France

### Abstract

We used a novel method based on allele-specific quantitative polymerase chain reaction (Intplex) for the analysis of circulating cell-free DNA (ccfDNA) to compare total ccfDNA and *KRAS*- or *BRAF*-mutated ccfDNA concentrations in blood samples from mice xenografted with the human SW620 colorectal cancer (CRC) cell line and from patients with CRC. Intplex enables single-copy detection of variant alleles down to a sensitivity of  $\geq 0.005$  mutant to wild-type ratio. The proportion of mutant allele corresponding to the percentage of tumor-derived ccfDNA was elevated in xenografted mice with *KRAS* homozygous mutation and varied highly from 0.13% to 68.7% in samples from mutation-positive CRC patients ( $n = 38$ ). Mutant ccfDNA alleles were quantified in the plasma of every patient at stages II/III and IV with a mean of 8.4% (median, 8.4%) and 21.8% (median, 12.4%), respectively. Twelve of 38 (31.6%) and 5 of 38 (13.2%) samples showed a mutation load higher than 25% and 50%, respectively. This suggests that an important part of ccfDNA may originate from tumor cells. In addition, we observed that tumor-derived (mutant) ccfDNA was more fragmented than ccfDNA from normal tissues. This observation suggests that the form of tumor-derived and normal ccfDNA could differ. Our approach revealed that allelic dilution is much less pronounced than previously stated, considerably facilitating the noninvasive molecular analysis of tumors.

*Translational Oncology* (2013) 6, 319–328

Address all correspondence to: Alain R. Thierry, PhD, Institut National de la Santé et de la Recherche Médicale, U896, Montpellier, F-34298, France. E-mail: alain.thierry@inserm.fr  
<sup>1</sup>F.M. is supported by a grant from the Centre National de la Recherche Scientifique (CNRS) and the Region of Languedoc-Roussillon (CNRS044406). The study was granted from the GEFLUC (DCMLP10-184, Montpellier, France). A.R.T. is supported by the Institut National de la Santé et de la Recherche Médicale (Montpellier, France).

<sup>2</sup>This article refers to supplementary materials, which are designated by Tables W1 to W3 and Figures W1 and W2 and are available online at [www.transonc.com](http://www.transonc.com).  
Received 29 November 2012; Revised 3 January 2013; Accepted 25 January 2013

## Introduction

KRAS is an essential activator within the signaling cascade induced by the activation of the *endothelial growth factor receptor (EGFR)* gene. KRAS plays a central role in tumor development by regulating the expression of the proteins that are involved in cell proliferation and survival, metastatic spread, and angiogenesis. *KRAS* point mutations lead to a constitutively active guanosine triphosphate (GTP)-bound protein that confers the signal to *BRAF* and the subsequent downstream activation of the mitogen-activated protein kinase (MAPK) pathway. The presence of some *KRAS* point mutations leads to its constitutively activation and renders the treatment of colorectal cancer (CRC) patients with potent inhibitors of EGFR, such as cetuximab and panitumumab, ineffective [1]. Therefore, all patients eligible for anti-EGFR treatments must first be tested for *KRAS* mutations (present in 35–45% of CRC cases) before starting such therapies. *BRAF* point mutations in CRC cells (8–14% of CRC cases) might also cause resistance to targeted therapies. *BRAF* and *KRAS* mutations are considered as mutually exclusive in CRC [2]. Although the detection of *BRAF* mutations is also associated with poorer prognosis [3,4], the *BRAF* mutational status has not been incorporated into the treatment guidelines in force because of conflicting results among studies. Currently, analysis of the *KRAS* mutational status of a patient is carried out from tumor sections by various methods including sequencing. It represents one of the first molecular assessments of personalized medicine in oncology. *BRAF V600E* mutation is examined in the case of a negative *KRAS* mutation status in several national guidelines, thus enlarging the targeted therapy-resistant patient population stratum.

Significant amounts of circulating cell-free DNA (ccfDNA) are present in the plasma of cancer patients [5,6]. As blood analysis of ccfDNA is easy to set up and relatively noninvasive, ccfDNA represents a very attractive tool for detecting the presence of mutations. ccfDNA dynamics can be easily modeled using xenografted mice [7,8]. Plasma ccfDNA in cancer patients may originate from three sources: 1) healthy normal cells, 2) tumor stromal cells, and 3) tumor cells [9]. A partial overlap in the ccfDNA level between healthy individuals and cancer patients has been observed in the literature [10,11]. Quantification of ccfDNA exclusively derived from tumor cells represents an obvious interest with regard to monitoring or following up tumor progression in the course of cancer patient management. Only a few reports have described the systematic quantification of tumor-derived ccfDNA [12–16] based on assays for quantifying ccfDNA harboring the point mutation that characterizes the tumor. Thus, mutant ccfDNA has been found previously as a tiny fraction of the total ccfDNA [13–15].

We have previously demonstrated that quantifying ccfDNA by quantitative polymerase chain reaction (Q-PCR) analysis is largely dependent on the target size [17]: The ccfDNA size pattern can discriminate plasma from CRC patients and from plasma from healthy individuals [18]. From these observations, we set up a Q-PCR-based method that demonstrated the unprecedented sensitivity and specificity of quantifying mutant ccfDNA. In this study, we determined the proportion of mutant (tumor cell-derived) alleles from ccfDNA analysis in a CRC mouse xenograft model and in 38 CRC patient plasma samples. The results are related to the as-yet-unknown contribution of the ccfDNA cell or tissue origins.

## Materials and Methods

### Cell Lines

The human colorectal adenocarcinoma HCT-116, SW620, LS174T, SW1116, and HT29, the human lung adenocarcinoma A549, and

the human pancreatic MiaPaca2 cell lines were obtained from ATCC (Manassas, VA). They were grown in RPMI 1640 supplemented with 10% fetal calf serum and 2 mmol/l L-glutamine at 37°C in a humidified atmosphere with 5% CO<sub>2</sub>.

### Mouse Xenograft Model

Female athymic nude mice (6–8 weeks of age,  $n = 8$ ) were xenografted with human SW620 CRC cells as previously described [18]. Three nude mice were not grafted and were used as controls. The mice were sacrificed using CO<sub>2</sub>. Blood collection and tumor weighing were carried out at different times post graft. All experiments were performed by an accredited person (Dr B. ROBERT, No. 34-156) and they complied with the current national and institutional regulations and ethical guidelines.

### Human Blood Samples

Blood samples were collected from patients ( $n = 38$ ) with CRC (metastatic or not), irrespective of their CRC stage or relapse (stage IV,  $n = 33$ ; stage III,  $n = 1$ ; stage II,  $n = 4$ ). CRC patients did not receive chemotherapy or radiotherapy for at least 1 month before the blood collection. The clinical features [Tumor Nodule Metastasis (TNM) staging] and the treatment for each CRC patient in this study before blood collection are summarized in Tables 1 and W1, respectively. Positive mutation status was retrospectively or prospectively carried out in tissue (primary tumor or metastasis) in the context of the standard management care of CRC patients. All plasma samples included in this study were analyzed correctly (100% success rate). Plasma analysis was performed in a blinded manner and only once for each of the 38 patients considered for treatment or surgery. Written, informed consent was obtained from all participants before the onset of the study. The protocols for the use of blood samples from healthy volunteers used in this study were approved by the “Etablissement Français du Sang” Ethics Committee (EFS-PM agreement: 21/PVNT/MTP/CNR14/2010-0029).

### Plasma Isolation and ccfDNA Extraction

Blood samples were collected in EDTA tubes: 2 ml of blood was collected from human patients and 0.8 to 1 ml from mice. The blood was centrifuged at 1200g at 4°C in a Heraeus Multifuge LR centrifuge for 10 minutes. The supernatants were isolated in sterile 1.5-ml Eppendorf tubes and centrifuged at 16,000g at 4°C for 10 minutes. Subsequently, the supernatants were either immediately handled for DNA extraction or stored at –80°C. ccfDNA was extracted from 1 ml of plasma using the QIAmp DNA Mini Blood Kit (Qiagen, Hilden, Germany) according to the “Blood and body fluid protocol.” DNA samples were kept at –20°C until use.

### ccfDNA Quantification by Q-PCR

The methodology and the data description were carried out according to the MIQE guidelines [19]. Q-PCR amplifications were carried out at least in duplicate in a 25- $\mu$ l reaction volume on a Chromo4 instrument using the MJ Opticon Monitor 3 software (Bio-Rad, Hercules, CA). Each PCR mixture was composed of 12.5  $\mu$ l of PCR mix (Bio-Rad Supermix SYBR Green), 2.5  $\mu$ l of each amplification primer (0.3 pmol/ $\mu$ l), 2.5  $\mu$ l of PCR-analyzed water, and 5  $\mu$ l of DNA extract. Thermal cycling consisted of three repeated steps: a 3-minute hot-start polymerase activation-denaturation step at 95°C followed by 40 repeated cycles at 95°C for 10 seconds and then at 60°C for 30 seconds. Melting curves were obtained by increasing the temperature from 55 to 90°C with a plate reading every 0.2°C.

**Table 1.** Determination by Q-PCR of the ccfDNA Concentration (refA) and of the Proportion of Mutant Allele (mA%) in Plasma Samples from CRC Patients with KRAS- or BRAF-Mutated Tumors.

Sample	TNM Status	Mutation	refA (ng/ml Plasma)	mA%
CRC1	T3N0M0	G13D	2.6	12.69
CRC2	T3N2M1	G12V	32.5	0.89
CRC3	T0N0M1	G12D	24.6	7.67
CRC4	T0N0M1	G12A	167	32.76
CRC5	T4N2M1	BRAF V600E	177.9	46.22
CRC6	T3N2M1	G12D	55.9	64
CRC7	T0N0M1	BRAF V600E	359.3	44.77
CRC8	T3N0M0	BRAF V600E	25.3	5
CRC9	T3N2M1	G13D	28.2	4.05
CRC10	T0N0M1	BRAF V600E	15.4	10
CRC11	T4N2M1	G12S	47.3	12.04
CRC12	T3N2M1	BRAF V600E	45.2	10.72
CRC13	T3N2M1	G12C	143.3	2.56
CRC14	T3N2M1	BRAF V600E	31	26.6
CRC15	T3N2M1	G12C	23.7	0.332
CRC16	T3N2M1	G13D	41.7	13.12
CRC17	T4N2M1	G12S	160.9	43.5
CRC18	T4N2M1	G12V	14.9	1.73
CRC19	T4N2M1	G13D	175.8	64.16
CRC20	T4N2M1	G13D	89.8	18
CRC21	T4N2M1	G12V	200.5	4.57
CRC22	T3N2M1	G13D	25.1	12.18
CRC23	T3N0M1	G13D	21	0.711
CRC24	T0N0M1	G12V	544	17.5
CRC25	T0N0M1	G12D	1386.9	36.6
CRC26	T3N2M1	G13D	42.2	4.15
CRC27	T4N1M0	G12S	29.4	8.36
CRC28	T3N0M0	G13D	13.1	6.62
CRC29	T3N0M1	G12V	13.6	6.59
CRC30	T4N0M1	G13D	10.3	56.36
CRC31	T4N0M1	G12A	25.1	8.5
CRC32	T4N0M1	G12V	6.2	68.77
CRC33	T4N0M0	G12A	23.9	9.26
CRC34	T4N0M1	G12D	47.1	9.51
CRC35	T4N0M1	G12D	36.1	29.18
CRC36	T4N0M1	G13D	87.2	56.91
CRC37	T3NxM1	G12V	6.7	5.05
CRC38	T3NxM1	G13D	220.7	0.13

Mutational status was confirmed by tumor section analysis as described in Materials and Methods section. TNM represents the Tumor Nodule Metastasis classification. refA corresponds to the total allele concentration (in ng/ml plasma) of a reference allele (Figure 1). mA% was calculated as the percentage of mutant allele from refA.

Serial dilutions of genomic DNA from human placenta cells (Sigma, Munich, Germany) were used as standard for quantification and their concentration and quality was assessed using a Nanodrop spectrophotometer (Thermo Scientific, Wilmington, DE). Each sample was analyzed in duplicate or in triplicate and each assay was repeated at least once. The ccfDNA concentrations obtained with each primer set were normalized to the precise concentration of a genomic DNA sample amplified using the same primer set. The coefficient of variation of the concentration value due to ccfDNA extraction and Q-PCR analysis was calculated as 24% from two experiments ( $n = 12$ ). Quantification of murine- or human-derived ccfDNA in our experimental mouse model was performed by using the primer systems described in Table W2.

**Intplex Mutation Analysis**

We established an allele-specific blocker [20] Q-PCR-based method specific for ccfDNA analysis (named Intplex) to enable the detection of point mutation and to determine mutant allele concentration. This method combined the use of 1) allele-specific Q-PCR with blocking 3'-phosphate-modified oligonucleotide [20], 2) low Tm primers with mutation in 3', 3) an integrated primer design, 4) routine internal positive and negative controls, and 5) optimal analytical procedures.

The blocking oligonucleotides were modified by adding a phosphate group in the 3' extremity to increase the specificity of Q-PCR by blocking the nonspecific extension of wild-type (WT) sequences. Mutational status was determined by detection of the specific amplification of the mutant sequence through melting analysis: only samples with amplification showing Tm within a 0.4°C range compared to the internal positive control from mutated cell line DNA was designated as positive for the mutation. The concentration was calculated from Cq detected by Q-PCR and a control standard curve on DNA of known concentration and copy number (Sigma-Aldrich). Each concentration of sample used for standard curve was controlled by nanodrop evaluation.

Intplex primer system design is presented in Figure 1. The concentration obtained when targeting the mutated sequence corresponds to the concentration of the alleles bearing the mutation (mA). The concentration obtained when targeting the WT sequence located at 300 bp from the position of the point mutation corresponds to total ccfDNA (WT + mutated ccfDNA) and is called refA. The proportion of mutant allele (mA%) was determined by quantifying the relative ratios between mA and refA (Figure 1).

We adapted Intplex for the detection of the KRAS hot-spot mutations at the 2nd exon (G12V, G12A, G12D, G12S, G12C, and G13D), which combined corresponds to 96% of KRAS-mutated tumors in CRC (Cosmic Sanger analysis), and also for the detection of the human BRAF 15th exon sequence containing the V600E point mutation, which corresponds to 97.8% of BRAF-mutated tumors in CRC (Cosmic Sanger analysis). The proportion of mutant allele (mA%) was determined for the fragments >60 to 64 bp for KRAS and >97 bp for BRAF (Figure 1).

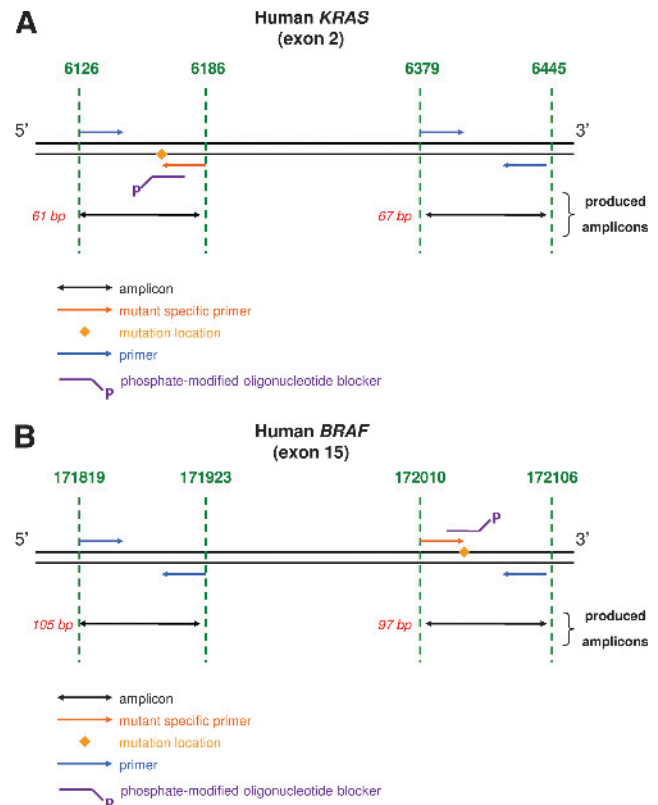


**Figure 1.** Primer designs used in the study: primers targeting a KRAS region (A) or a BRAF region (B) for quantifying ccfDNA WT and mutated concentrations.

Positive control DNA was extracted from cell lines bearing the *KRAS* and *BRAF* mutations. The respective correspondence between cell lines and the corresponding mutation was further detailed: HCT-116 for the G13D *KRAS* mutation, SW620 for the G12V *KRAS* mutation, A549 for the G12S *KRAS* mutation, LS174T for the G12D *KRAS* mutation, MiaPaca2 for the G12C mutation, SW1116 for the G12A *KRAS* mutation, and HT29 for the V600E *BRAF* mutation.

Every mutational status, summarized in Table 1, was further validated by comparing it with that obtained from the genomic DNA analysis of tumor sections by either sequencing (>50% of tumor cells) or by high resolution melt (HRM) and pyrosequencing (20% to 50% of tumor cells) [21].

### Sensitivity and Specificity Analysis of the Quantification of Mutant ccfDNA

Evaluation of the sensitivity level of our method was first conducted on genomic DNA. DNA from cells harboring a specific mutation was serially diluted six times into high concentrated WT genomic DNA from human placenta (Sigma-Aldrich) up to dilution of 0.2 mutated copies in 20,000 copies (1/100,000 ratio). All the experimental points were obtained in triplicate.

### Primer Design

The sequences and characteristics of the selected primers are presented in Table W2. The primers were designed using the Primer 3 software and all sequences were checked for self-molecular or inter-molecular annealing with nucleic acid folding software (mfold and oligoAnalyzer 1.2). We performed local alignment analyses with the BLAST program to confirm the specificity of the designed primers. Oligonucleotides were synthesized and purified on high performance liquid chromatography (HPLC) by Eurofins (Ebersberg, Germany) and quality control of the oligonucleotides was performed by matrix-assisted laser desorption ionization–time of flight (MALDI-TOF).

### ccfDNA Size Allele Analysis

We used a set of primers that amplifies targets of increasing size (82, 138, 200, 300, 355, and 390 bp) within the hot-spot region of the *KRAS* gene (codons 12 and 13 of exon 2) and in which the forward primer of each primer pair specifically targets a point mutation of this region or the WT sequence (Table W2 and Figure W1). Therefore, the concentration of the allele bearing either the point mutation (mA) or not (wtA) was directly compared to the ccfDNA fragment size. The plasma of the CRC patients with *KRAS* G13D (CRC1) and *KRAS* G12D (CRC3 and CRC6) mutations was examined. The efficiency of

the PCR primer system was normalized with known amount of genomic DNA (in ng) from cell lines harboring *KRAS* G12D (LS174T) or G13D (HCT116) mutations.

### Integrity Index Analyses

Intplex method allowed calculation of the ccfDNA integrity index. The degree of ccfDNA integrity was assessed by calculating an index we termed the DNA integrity index (DII). The DII was determined by calculating the ratio of the concentration determined by using the primer set amplifying the large (circa 300 bp) target to the concentration determined by using the primer set amplifying the short (<100 bp) target (Figure 1).

## Results

### Sensitive and Specific Quantification of Mutant ccfDNA by a Q-PCR–Based Method

We set up a Q-PCR method combining several refinements for allele-specific discrimination and a primer system design specific to ccfDNA. The integrated primer design of our test involves amplification at the extremities of a 300-bp region of two shorter regions of the same size (in the range of 60–100 bp,  $\pm 10\%$ ), one corresponding to a mutated sequence and another to a WT sequence (Figure 1, A and B). We demonstrated previously the crucial importance of the primer set design by demonstrating that ccfDNA quantification by Q-PCR is much higher and more accurate when amplifying regions shorter than 100 bp [18]. Varying PCR target size of both short amplicons of more than 10% generates detectable differences between the determined respective ccfDNA amounts. Serial dilutions of mutant DNA to WT ratio revealed detection of the mutant at a level of 1/25,000 for each *KRAS* and *BRAF* mutation, as illustrated in Figure W2. Intplex enables single-copy detection of variant alleles down to a sensitivity of  $\geq 0.005\%$  mutant to WT ratio.

As a result, this system design allows the accurate determination of the percentage of mutant allele (mA%). In this study, the lowest mA% found in mCRC plasma was 0.13% (Table 1).

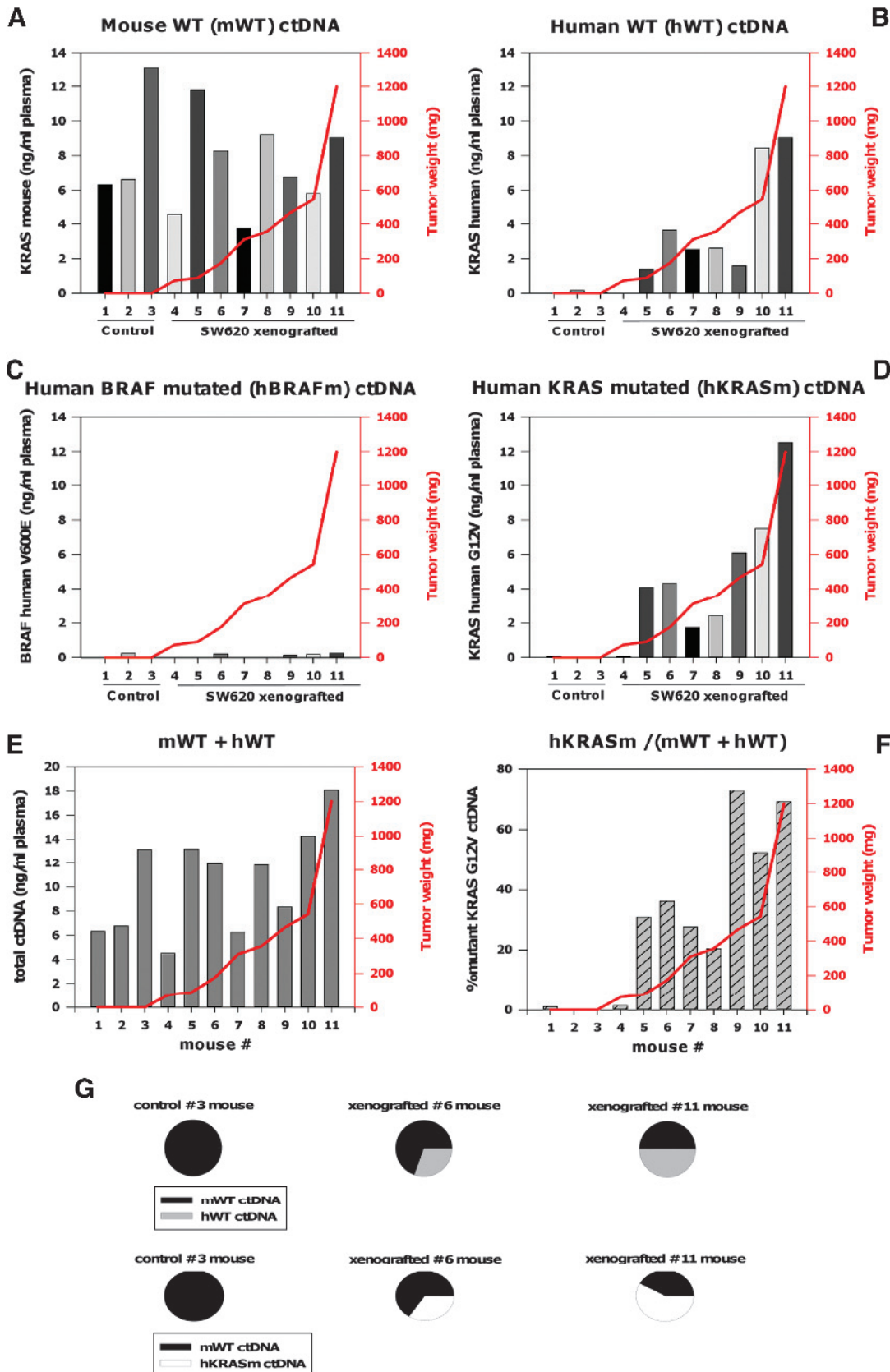
### Up to 63% of Total ccfDNA in Mice Xenografted with Cells Harboring a Homozygous *KRAS* G12V Mutation Originates from Tumors

We used athymic nude mice xenografted with human SW620 CRC cells to clearly distinguish between nontumor-derived (mouse origin) and mutated or nonmutated tumor-derived (human origin) ccfDNA (Figure 2 and Table W3). These cells were homozygous for the *KRAS*

**Figure 2.** Quantification by Q-PCR of ccfDNA derived from malignant and nonmalignant cells in the mouse model. Tumor weight is represented by the red curve (right axis). (A) Concentration of ccfDNA derived from mouse (normal) cells (mWT ccfDNA) in control (not grafted) mice (Mouse Nos. 1–3) and in athymic nude mice (Mouse Nos. 4–11) xenografted with the SW620 colorectal human cells, determined using a primer set targeting a mouse *KRAS* second intron WT sequence (Table W2). (B) Concentration of ccfDNA derived from human cells (hWT ccfDNA) using a primer set targeting a human *KRAS* second intron WT sequence. (C) Concentration of ccfDNA derived from human cells (h*BRAF*m ccfDNA) using a primer set targeting a human *BRAF* 15th exon sequence containing the V600E point mutation (Table W2). (D) Concentration of ccfDNA derived from human cells (h*KRAS*m ccfDNA) using a primer set targeting a human *KRAS* second exon sequence that contains the G12V point mutation. (E) Concentration of total ccfDNA (mWT ccfDNA + hWT ccfDNA). (F) Proportion of h*KRAS*m ccfDNA in total ccfDNA. (G) Proportion of tumor-derived ccfDNA and *KRAS*-mutated tumor-derived ccfDNA versus nontumor-derived ccfDNA expressed as the percentage of the total ccfDNA (derived from both mouse and human cells as quantified here). Concentration values are described in Table W3.

G12V mutation. We first confirmed several observations that we have described previously [18]: 1) the nontumor-derived ccfDNA amount in mouse plasma (Figure 2A) did not vary with tumor size, 2) the control mouse ccfDNA amount (mean,  $8.6 \pm 3.8$  ng/ml; median,

6.6 ng/ml) was similar to the nontumor-derived ccfDNA amount (mean,  $7.4 \pm 2.6$  ng/ml; median, 7.5 ng/ml; Figure 2A), 3) the tumor-derived ccfDNA amount appeared to increase with tumor size (Figure 2, B and D), and 4) no ccfDNA was detected when targeting



the *BRAF* V600E point mutation (Figure 2C), highlighting the high specificity of our analysis to quantify and detect the presence of ccfDNA alleles with a specific point mutation.

Moreover, our data showed that the amount of the ccfDNA derived from the tumor, as determined when targeting the human *KRAS* second intron, was found to be somewhat similar to the amount of human *KRAS* second exon G12V-mutated ccfDNA (Figure 2, B and D). This observation was consistent both with the clonogenic property of the SW620 cells used for the xenografts and with the same allele being carried by each member of the pair of homologous chromosomes in these cells (homozygous mutation). In addition, this demonstrates consequently that our method for determining the concentration of *KRAS* second exon G12V-mutated ccfDNA was accurate. Tumor-derived ccfDNA represented a prevalent proportion (35–44%) of the total ccfDNA concentration (derived from both mouse and human cells, as quantified in this study) in mice bearing tumors between 100 and 500 mg in weight; this amount ranged from 44% to 63% in mice with 500 to 1200 mg of tumors (Figure 2, E–G). Hence, we concluded that more than half of the total concentration of ccfDNA in xenografted mice may be derived from the tumor, which can be quantified by detecting *KRAS*-mutant ccfDNA.

#### 0.13% to 69% of *KRAS*-Mutant Allele Was Observed in ccfDNA from the Plasma of *KRAS*-Mutated CRC Patients

On the basis of these results, we examined the quantification of selected *KRAS*- and *BRAF*-mutated ccfDNA in the plasma of CRC patients. Table 1 and Figure 3 present the mutation detection and the percentage of mutated ccfDNA that we found in 38 plasma samples. This number of *KRAS/BRAF*-mutated samples could correspond to a nonselected cohort of 85 to 95 (negative and positive) CRC patient blood samples. The mutational status of all samples was further validated by comparing it with that obtained from the genomic DNA analysis of the tumor section either by sequencing or by HRM and pyrosequenc-

ing. Hence, mutant ccfDNA alleles could be quantified in the plasma of every patient at stages II, III, and IV (Table 1). The proportion of mutated ccfDNA alleles varied from 0.13% to 68.8% (mean, 20.05%; median, 10.36%) and, more precisely, at stages II and III (mean, 8.39%; median, 8.36%;  $n = 5$ ) and at stage IV (mean, 21.81%; median, 12.04%;  $n = 33$ ). Note that we found six plasma samples with 5% to 46.22% ccfDNA bearing the *BRAF* V600E point mutation.

#### The *KRAS*-Mutated and WT ccfDNA Fragment Size Profiles Markedly Differ

We observed previously that the total ccfDNA from the CRC patients' plasma is much more fragmented than that from healthy individuals [18]. Since our preliminary results revealed a high proportion of tumor-derived ccfDNA, we examined its size pattern in comparison with nontumor-derived ccfDNA from CRC patients (Figure 4). The size profile of the ccfDNA fragments bearing a mutation detected in CRC6, CRC3, and CRC1 plasma was similar. Similarity in the size profile was also observed in these three CRC plasmas when detecting the WT sequence. In all cases, the concentration of ccfDNA was correlated inversely with the amplicon size. It appeared very low or non-detectable when targeting 355 and 390 bp. Note that the sum of wtA and mA was 92%, 54%, and 146% of refA (Figure 4), suggesting a somewhat equivalency between wtA + mA and refA, inasmuch as the coefficient of variation of the plasma ccfDNA concentration as determined by our method was calculated as 24%.

Subsequently, we determined the percentage of mutant ccfDNA (mA%) relative to refA by using the primer set described in Figure 1B. mA% was 26.6%, 17.4%, and 20.6% in CRC6, CRC3, and CRC1, respectively (Figure 5), which confirmed the results determined with the primer set that amplified two 60-bp sequences in the same region of the *KRAS* exon 2 (Figure 1 and Table 1). Schmidt and Diehl [22] found that high fragmentation was not due to the storage conditions or the procedure used to prepare the samples.

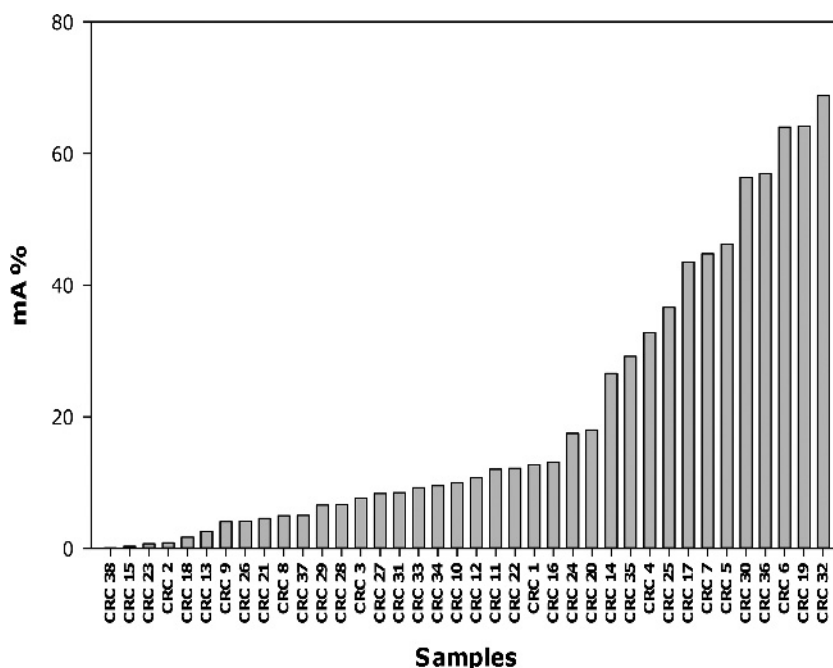


**Figure 3.** Histogram of the proportion of mutant allele (mA%) in plasma samples from CRC patients with *KRAS*- or *BRAF*-mutated tumor.

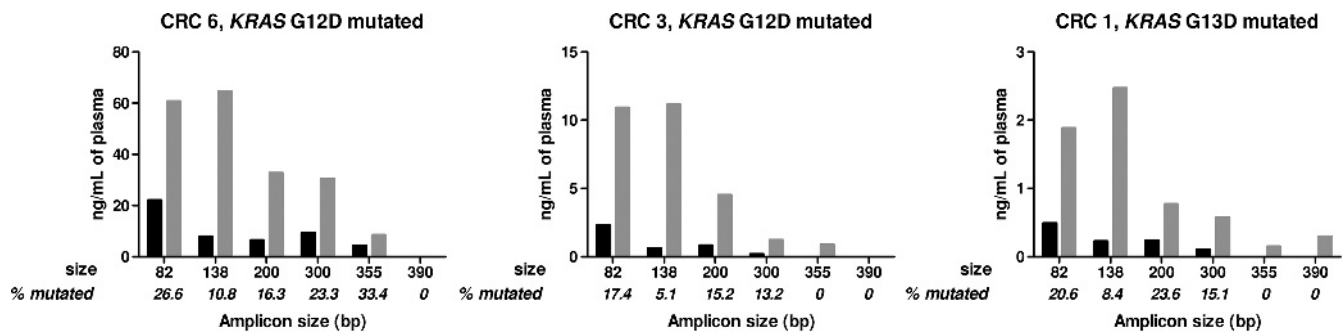


**Figure 4.** Comparison of the ccfDNA fragment size distribution of mutant (black bars) and nonmutant (gray bars) ccfDNA in plasma samples from patients with CRC bearing a point mutation in the *KRAS* exon 2. Data are expressed as ng of ccfDNA/ml plasma. ccfDNA from the plasma of patients CRC6 (*KRAS* G12D), CRC3 (*KRAS* G12D), and CRC1 (*KRAS* G13D) was quantified by amplifying *KRAS* exon 2 sequences of increasing size (82, 138, 200, 300, 355, and 390 bp; Figure W1 and Table W2). Detection of the resulting amplicons of various sizes enables quantification of the size fractions of ccfDNA contained in a mononucleosome (180–200 bp) and a dinucleosome (360–380 bp) [27,28]. Plasma of CRC6, CRC3, and CRC1 were chosen because of their high total ccfDNA content and high mutant ccfDNA proportion (Table 1).

Furthermore, among the 82- to 138-bp ccfDNA fragments, very few WT fragments (Table 2) were observed in contrast to the very high proportion of mutant fragments (70.1%, 74.0%, and 89.3% in CRC6, CRC3, and CRC1, respectively; Figure 5). This was confirmed by using the plasma sample of another CRC patient harboring the *KRAS* G12V mutation (CRC2) in which 52.1% of the 82- to 138-bp ccfDNA fragments carried the mutation (Figure 5). By quantifying the proportion of *KRAS*-mutated ccfDNA, we demonstrated that tumor-derived ccfDNA could be discriminated from ccfDNA originating from non-malignant cells, assuming that the mutant allele is in great excess among all tumor malignant cells [23].

## Discussion

### *The Mutation Loads in the Xenografted Mouse Animal Model and in CRC Plasma Differ Markedly*

ccfDNA analysis showed the very high proportion of mutant allele (up to 63%) present in xenografted mice and demonstrated that the mutant tumor-derived ccfDNA amount corresponds to the total tumor-derived ccfDNA amount. This suggests tumor cell clonogenicity and a very low proportion of tumor microenvironment surrounding cells. These observations highlight some of the crucial differences between this experimental mouse model and the clinical setting when compared with our data on CRC plasma samples, which showed, in some cases, a very low proportion of the mutant allele.

### *The Mutation Load in CRC Patients' Plasma Is Highly Variable*

Only two papers from the same group based on a cohort study and another two based on one case report have reported previously the examination of the proportion of mutant ccfDNA alleles among total circulating DNA alleles. Diehl et al. [13–15] developed a highly sensitive approach (BEAMing) to detect and quantify ccfDNA harboring *APC* mutations in CRC patients' plasma samples [13]. Assuming that they calculated the mutant *APC* fragment percentage as the mA% value, they detected lower amounts of mutant allele (median of 0.04% for samples from patients with Dukes A,  $n = 8$ ; 1.28% for patients with Dukes B,  $n = 8$ ; and 8.05% for patients with Dukes D,  $n = 6$ , cancers) in comparison with our data. In another study, this group

evaluated the median percentage of mutant allele as 0.18% in plasma from 16 Dukes D CRC patients [14,15]. Furthermore, only 0.3% of ccfDNA with the *KRAS* G12V mutation was detected in the plasma sample from a patient with metastatic CRC using this technique [16]. The high mA% variation observed by this group was confirmed in our study, despite the higher median values we obtained. In particular, our study revealed, for the first time, several cases (5 of 38) where more than half of total ccfDNA amount was mutated (Figure 5). This observation indicated that, in some cases, ccfDNA may originate mainly from tumor cells. Twelve of 38 (31.6%) samples showed a mutation load higher than 25% (Figure 4). As a consequence, the tumor-derived ccfDNA did not correspond to “a tiny fraction” as previously stated [13–16] and it may not have derived mainly from stroma cells.

The higher level of mutation load as observed here may be due to the use of targeting low size sequence (<100 bp) in exon 2 and exon 15 of *KRAS* and *BRAF*, respectively. Targeting low size sequence for ccfDNA was based on previous work [18] in which a ccfDNA size distribution study indicated a much higher (four- to six-fold) efficacy in detecting WT intron fragments (total ccfDNA). The approach of comparing amplification data of a specific sequence with another sequence of a similar target size ( $\pm 10$  bp) within a 300-bp region, as carried out here (Figure 1), enabled the direct comparison between the concentration of the mutant and the WT *KRAS* sequence (Figure 5) and, subsequently, accurate determination of mutation load (Figure 3). In addition, the combination of allele-specific priming, blocking of WT unspecific amplification, and melting analysis provides unsurpassed sensitivity and specificity for a Q-PCR-based method. Intplex can be adapted to all point mutations of interest.

The higher percentage of mutant ccfDNA detected with our Q-PCR method may be due to the use of the *KRAS* and the *BRAF* mutations as biomarkers and also to our Q-PCR method. Its use revealed that allelic dilution appears less pronounced than previously stated [13–15], easing the detection of resistance-associated point mutations and the quantification of mutant ccfDNA alleles. Alternatively to the hypothesis of Diehl and Vogelstein [13], the observation of mA% higher than 25% in more than one-third of the plasma samples provides evidence that ccfDNA does not originate only from microenvironment cells but rather that a significant proportion of ccfDNA could be tumor derived. It was shown that phagocytosis by macrophages or other scavenger cells of apoptotic or necrotic neoplastic cells



could lead to DNA release in the circulation of patients with cancer [24]. This seems to occur especially in invasive tumors, which generally contain large regions of necrosis due principally to hypoxia. Interestingly, the CRC tumor was among the tumors with a higher cell loss factor (94–98%) [25], which might explain the high ccfDNA level observed in CRC patients.

mA% was highly variable (0.13–68.77%), as determined from ccfDNA by Intplex among the positive *KRAS* or *BRAF* mutational status CRC plasma samples ( $n = 38$ ). This raises crucial questioning

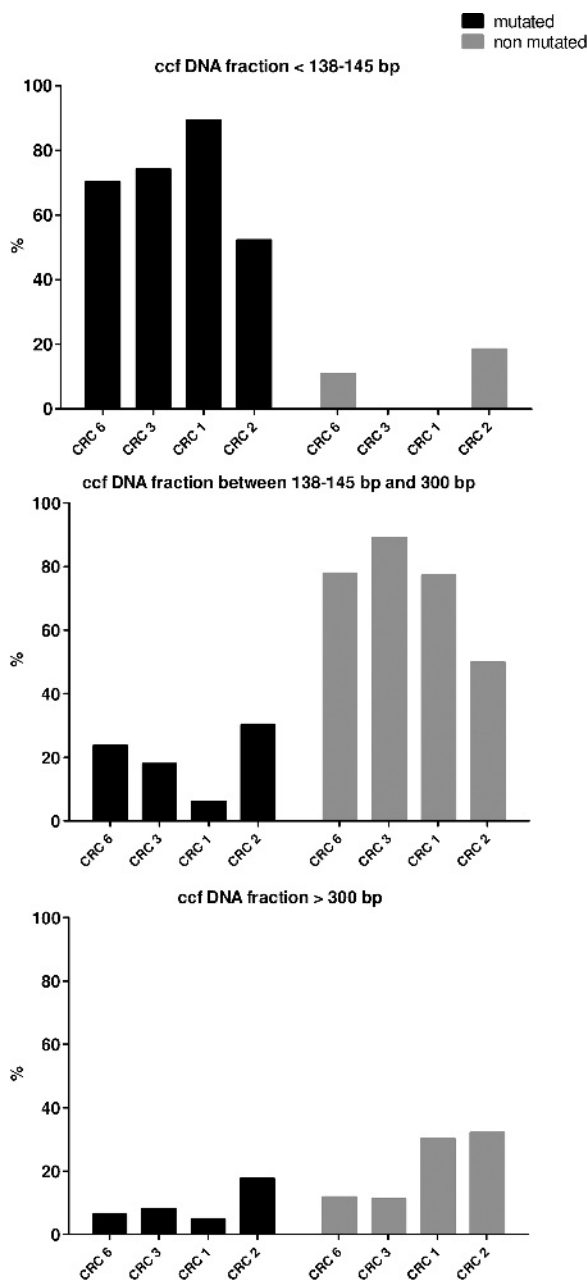


**Figure 5.** Histogram representation of the various parameters indicative of ccfDNA fragment size pattern. Size fraction is expressed as a percentage of the highest value obtained in each size set. *KRAS* second exon primer systems enable quantification of mutant ccfDNA and ccfDNA harboring the WT sequence at the mutation location, respectively. Numbers under the histograms: 6, 3, 1, and 2, plasma from CRC patients with a positive mutational status for *KRAS* (CRC1–3 and CRC6).

**Table 2.** Data of the Various Parameters Indicative of ccfDNA Fragment Size Pattern.

Samples	Q-PCR Target	Fraction Concentration (ng/ml Plasma)			DII
		<138	138 > x > 300	>300	
CRC6	Mutant <i>KRAS</i> second exon	18.75	6.27	1.68	0.06
CRC3	Mutant <i>KRAS</i> second exon	1.69	0.41	0.18	0.08
CRC1	Mutant <i>KRAS</i> second exon	0.26	0.12	0.09	0.05
CRC2	Mutant <i>KRAS</i> second exon	2.25	1.3	0.76	0.18
CRC6	WT <i>KRAS</i> second exon	8.14	59.04	8.91	0.12
CRC3	WT <i>KRAS</i> second exon	0	9.91	1.21	0.11
CRC1	WT <i>KRAS</i> second exon	0	1.9	0.56	0.3
CRC2	WT <i>KRAS</i> second exon	7.27	19.69	12.71	0.32

The proportion of ccfDNA fragment <138 bp was determined by subtracting the concentration determined by using the primer set amplifying the 82-bp target from the concentration determined by using the primer set amplifying the 138-bp target (138 bp – 82 bp). Negative values are expressed arbitrarily as 0. The ccfDNA integrity index (DII) was determined by calculating the ratio of the concentration determined using the primer set amplifying the 300-bp target to the concentration determined using the primer set amplifying the 82-bp target.

about the cell origin of ccfDNA release, tumor cell composition, and mutant allele specific imbalance. In CRC patients, we can discriminate three cells from which the release of ccfDNA originates: 1) malignant tumor cells, 2) tumor microenvironment cells (stromal, epithelial, or inflammatory cells), and 3) nontumor-derived cells, which produce the basal ccfDNA level in healthy individuals (about 5 ng/ml, [18]). The highest mA% (68.77%) is more than 500-fold greater than the lowest mA% (0.13%) observed. As it seems unlikely that the proportion of the microenvironment cells reaches up to more than 90%, the low mA% observed in a significant proportion of the plasma samples (for instance, 18/38 being lower than 10%) was not only due to a low malignant cell proportion but also to poor tumor cell clonogenicity. West et al. [26] demonstrated that the median proportion of cells from primary CRC tumors was 57.1% (interquartile range from 47.4% to 66.4%) and 9% at the lowest in pT1 stage cancer.

The proportion of mutated tumor cells within a tumor may be expressed by the mutation load, which can be determined by quantifying the number of mutated cells in a tumor section [23,26] or by quantifying the mutant alleles from circulating DNA, as performed in this study. It depends on the mutation zygosity status, being directly equivalent to the mutant allele percentage in case of homozygosity or being twice as much as the mutant allele percentage in case of heterozygosity. We determined through the Cosmic Sanger database and several reports that 25% and none of the colorectal adenocarcinoma tumor samples that tested positive showed a *KRAS* and *BRAF* homozygous mutation, respectively. Since the zygosity status of the patient tumors was unknown in our study, we were unable to quantify precisely their mutation load. Nevertheless, we can assume that the five CRC plasma samples showing a mutant allele percentage superior to 50% correspond to a tumor-bearing *KRAS* homozygous mutation. Given the heterozygosity of the *BRAF* 600E mutation, the allele mutation load is equivalent to half of the genome-equivalent mutation load, and as a result, the proportion of malignant cells at least ranged from 10% to 92.4%.

Our data might suggest a very high variation in the proportion of malignant cells in colorectal tumors and/or low tumor cell clonogenicity. However, the direct relationship between these data and the proportion of malignant cells is currently uncertain as the mechanism of ccfDNA release determines the yield (necrosis, apoptosis, or active release). Therefore, interindividual comparison of the proportion of mutant allele determined from circulating DNA could appear somewhat more difficult to interpret; however, this parameter could be an efficient biomarker for monitoring or following up CRC patients

and could be combined with size fraction analysis, as demonstrated in this study, to provide a deeper examination toward this goal.

### ccfDNA Size Fraction Analysis Characterizes Tumor-Derived ccfDNA

ccfDNA is thought to be released through various mechanisms such as necrosis, phagocytosis, apoptosis, or active release [27]. ccfDNA seems to be present in the circulation, especially in the form of complexes (through electrostatic bonds) with cell constituents (mononucleosomes or oligonucleosomes or nucleolipoproteins, [28,29]), or inserted in apoptotic vesicles that make it relatively stable. As apoptosis leads to high internucleosomal DNA fragmentation, fragments as small as 180 to 200 bp (the length of mononucleosome DNA) may be found following this release mechanism [27,28]. Apoptosis results to the release of shorter fragments compared to necrosis or phagocytosis (larger than 10,000 bp, [13]); therefore, the estimation of ccfDNA fragmentation could provide evidence on the ccfDNA release mechanism.

To specify cancer patients' ccfDNA and study its origin, previous studies have evaluated their fragmentation level. However, as stated by Jung et al. [30], experimental bias has led to large discrepancies when drawing general conclusions. Given the ability to quantifying mutant ccfDNA in this work, we studied various fragmentation indexes. Hence, in addition to the integrity index (corresponding to the proportion of DNA longer than the length of the mononucleosome DNA among the total ccfDNA) as previously examined [6,31], the proportion of various ccfDNA size fractions of the plasma from four CRC patients with a *KRAS* point mutation were determined (Figure 5). In CRC6, CRC3, CRC1, and CRC2 samples, preliminary results indicate that mutant ccfDNA was composed mostly of fragments <138 bp, while nonmutant ccfDNA was mostly constituted of fragments in the 138- to 300-bp range and very few fragments <138 bp. Conversely, Schmidt and Diehl [22] recently observed that mutant ccfDNA has almost no influence on DNA integrity, indicating that mutant ccfDNA presents a minor fraction of the total ccfDNA. This highlights the numerous discrepancies found in the literature on ccfDNA in cancer patients [30]; in this regard, we proved herein that careful methodology design with better knowledge of the ccfDNA structure would provide a more accurate observation.

Altogether, our data suggest that ccfDNA deriving from normal tissue or CRC patient tumors vary in their form, and consequently, their mechanism of release might be different. It is difficult to hypothesize on the high fragmentation of CRC tumor cell-derived ccfDNA, which could result in the release of either internucleosomal breaks, as a result of apoptosis, or large-sized ccfDNA, subsequent to necrosis or phagocytosis [28]. Nevertheless, these data indicate that the specific detection of *KRAS*-mutated ccfDNA enables its discrimination from the WT ccfDNA through the analysis of the ccfDNA fragment size profile. In addition, size fraction analysis could give information about the nature of the ccfDNA release mechanism. Size fraction analysis should be further studied by using a large cohort to validate our results and to determine whether it might be generalized for the analysis of other gene mutations.

### Clinical Implications and Perspectives

In addition to the diagnosis and monitoring of CRC patients, close indication of tumor evolution through the quantification of tumor (or mutant) ccfDNA by blood testing could allow the control and adaptation of chemotherapy or radiotherapy. mA% determination by ccfDNA analysis should be further examined in a large cohort

to study whether an mA% threshold could be defined under which the use of targeted therapy could be beneficial. Patient monitoring by examining *KRAS/BRAF*-mutant ccfDNA would be reduced to about half of CRC cases; nevertheless, analyzing ccfDNA-bearing mutations on other genes is likely in CRC as well as in other cancers. Determination of the mutation load might be of great interest: A recent study demonstrated that a low proportion of malignant cells compared to epithelial and stromal cells in CRC tumors is related to poor cancer survival [26]. Prospective trials should further investigate the clinical impact of this parameter and aim to evaluate whether it might also serve as a prognostic biomarker. Targeting highly fragmented ccfDNA revealed high level of mutant ccfDNA in a significant proportion of CRC plasmas. This provides clues for monitoring cancer progression with the aim of developing personalized treatment and to better circumscribe the potential biologic roles of ccfDNA-bearing specific oncogene point mutations.

### Acknowledgments

We are grateful to Brigitte Gillet, Virginie Lorient, and Michelle Nouaille for clinical help and assistance. We thank Jacques Robert and Julie Dubois for helpful discussion. We also thank Fanny Rolet for her assistance with plasma ccfDNA analysis, Béatrice Orsetti for her help with nanodrop measurements, and Leigh Kamraoui for English editing.

### References

- Lievre A, Bachet JB, Boige V, Cayre A, Le Corre D, Buc E, Ychou M, Bouche O, Landi B, Louvet C, et al. (2008). *KRAS* mutations as an independent prognostic factor in patients with advanced colorectal cancer treated with cetuximab. *J Clin Oncol* **26**, 374–379.
- Deng G, Bell I, Crawley S, Gum J, Terdiman JP, Allen BA, Truta B, Sleisenger MH, and Kim YS (2004). *BRAF* mutation is frequently present in sporadic colorectal cancer with methylated hMLH1, but not in hereditary nonpolyposis colorectal cancer. *Clin Cancer Res* **10**, 191–195.
- Corcoran RB, Dias-Santagata D, Bergethon K, Iafrate AJ, Settleman J, and Engelman JA (2010). *BRAF* gene amplification can promote acquired resistance to MEK inhibitors in cancer cells harboring the *BRAF* V600E mutation. *Sci Signal* **3**, ra84.
- Lea A, Allingham-Hawkins D, and Levine S (2010). *BRAF* p.Val600Glu (V600E) testing for assessment of treatment options in metastatic colorectal cancer. *PLoS Curr* **2**, RRN1187.
- Stroun M, Anker P, Maurice P, Lyautey J, Lederrey C, and Beljanski M (1989). Neoplastic characteristics of the DNA found in the plasma of cancer patients. *Oncology* **46**, 318–322.
- Mead R, Duku M, Bhandari P, and Cree IA (2011). Circulating tumour markers can define patients with normal colons, benign polyps, and cancers. *Br J Cancer* **105**, 239–245.
- Kamat AA, Bischoff FZ, Dang D, Baldwin MF, Han LY, Lin YG, Merritt WM, Landen CN Jr, Lu C, Gershenson DM, et al. (2006). Circulating cell-free DNA: a novel biomarker for response to therapy in ovarian carcinoma. *Cancer Biol Ther* **5**, 1369–1374.
- Rago C, Huso DL, Diehl F, Karim B, Liu G, Papadopoulos N, Samuels Y, Velculescu VE, Vogelstein B, Kinzler KW, et al. (2007). Serial assessment of human tumor burdens in mice by the analysis of circulating DNA. *Cancer Res* **67**, 9364–9370.
- Schwarzenbach H, Hoon DS, and Pantel K (2011). Cell-free nucleic acids as biomarkers in cancer patients. *Nat Rev Cancer* **11**, 426–437.
- Gormally E, Hainaut P, Caboux E, Airoldi L, Autrup H, Malaveille C, Dunning A, Garte S, Matullo G, Overvad K, et al. (2004). Amount of DNA in plasma and cancer risk: a prospective study. *Int J Cancer* **111**, 746–749.
- Fratini M, Gallino G, Signoroni S, Balestra D, Lusa L, Battaglia L, Sozzi G, Bertario L, Leo E, Pilotti S, et al. (2008). Quantitative and qualitative characterization of plasma DNA identifies primary and recurrent colorectal cancer. *Cancer Lett* **263**, 170–181.
- Leary RJ, Kinde I, Diehl F, Schmidt K, Clouser C, Duncan C, Antipova A, Lee C, McKernan K, De La Vega FM, et al. (2010). Development of personalized tumor biomarkers using massively parallel sequencing. *Sci Transl Med* **2**, 20ra14.

- [13] Diehl F, Li M, Dressman D, He Y, Shen D, Szabo S, Diaz LA Jr, Goodman SN, David KA, Juhl H, et al. (2005). Detection and quantification of mutations in the plasma of patients with colorectal tumors. *Proc Natl Acad Sci USA* **102**, 16368–16373.
- [14] Diehl F, Schmidt K, Choti MA, Romans K, Goodman S, Li M, Thornton K, Agrawal N, Sokoll L, Szabo SA, et al. (2008). Circulating mutant DNA to assess tumor dynamics. *Nat Med* **14**, 985–990.
- [15] Diehl F, Schmidt K, Durkee KH, Moore KJ, Goodman SN, Shuber AP, Kinzler KW, and Vogelstein B (2008). Analysis of mutations in DNA isolated from plasma and stool of colorectal cancer patients. *Gastroenterology* **135**, 489–498.
- [16] Holdhoff M, Schmidt K, Donehower R, and Diaz LA Jr (2009). Analysis of circulating tumor DNA to confirm somatic KRAS mutations. *J Natl Cancer Inst* **101**, 1284–1285.
- [17] Thierry AR, Moulriere F, Gongora C, Ollier J, Robert B, Ychou M, Del Rio M, and Molina F (2010). Origin and quantification of circulating DNA in mice with human colorectal cancer xenografts. *Nucleic Acids Res* **38**, 6159–6175.
- [18] Moulriere F, Robert B, Arnau Peyrotte E, Del Rio M, Ychou M, Molina F, Gongora C, and Thierry AR (2011). High fragmentation characterizes tumour-derived circulating DNA. *PLoS One* **6**, e23418.
- [19] Bustin SA, Benes V, Garson JA, Hellemans J, Huggett J, Kubista M, Mueller R, Nolan T, Pfaffl MW, Shipley GL, et al. (2009). The MIQE guidelines: minimum information for publication of quantitative real-time PCR experiments. *Clin Chem* **55**, 611–622.
- [20] Morlan J, Baker J, and Sinicropi D (2009). Mutation detection by real-time PCR: a simple, robust and highly selective method. *PLoS One* **4**, e4584.
- [21] Lopez-Crapez E, Mineur L, Emptas H, and Lamy PJ (2010). KRAS status analysis and anti-EGFR therapies: is comprehensiveness a biologist's fancy or a clinical necessity? *Br J Cancer* **102**, 1074–1075; author reply 1076–1077.
- [22] Schmidt K and Diehl F (2007). A blood-based DNA test for colorectal cancer screening. *Discov Med* **7**, 7–12.
- [23] Soh J, Okumura N, Lockwood WW, Yamamoto H, Shigematsu H, Zhang W, Chari R, Shames DS, Tang X, MacAulay C, et al. (2009). Oncogene mutations, copy number gains and mutant allele specific imbalance (MASI) frequently occur together in tumor cells. *PLoS One* **4**, e7464.
- [24] Choi JJ, Reich CF III, and Pisetsky DS (2005). The role of macrophages in the *in vitro* generation of extracellular DNA from apoptotic and necrotic cells. *Immunology* **115**, 55–62.
- [25] Ota DM and Drewinko B (1985). Growth kinetics of human colorectal carcinoma. *Cancer Res* **45**, 2128–2131.
- [26] West NP, Dattani M, McShane P, Hutchins G, Grabsch J, Mueller W, Treanor D, Quirke P, and Grabsch H (2010). The proportion of tumour cells is an independent predictor for survival in colorectal cancer patients. *Br J Cancer* **102**, 1519–1523.
- [27] Jahr S, Hentze H, Englisch S, Hardt D, Fackelmayer FO, Hesch RD, and Knippers R (2001). DNA fragments in the blood plasma of cancer patients: quantitations and evidence for their origin from apoptotic and necrotic cells. *Cancer Res* **61**, 1659–1665.
- [28] Deligezer U, Erten N, Akisik EE, and Dalay N (2006). Circulating fragmented nucleosomal DNA and caspase-3 mRNA in patients with lymphoma and myeloma. *Exp Mol Pathol* **80**, 72–76.
- [29] Gahan PB and Stroun M (2010). The virtosome—a novel cytosolic informative entity and intercellular messenger. *Cell Biochem Funct* **28**, 529–538.
- [30] Jung K, Fleischhacker M, and Rabien A (2010). Cell-free DNA in the blood as a solid tumor biomarker—a critical appraisal of the literature. *Clin Chim Acta* **411**, 1611–1624.
- [31] Ellinger J, Wittkamp V, Albers P, Perabo FG, Mueller SC, von Ruecker A, and Bastian PJ (2009). Cell-free circulating DNA: diagnostic value in patients with testicular germ cell cancer. *J Urol* **181**, 363–371.

**Table W1.** Treatment Received for each CRC Patient before the Blood Collection.

Sample	Treatment before Blood Collection
CRC1	CT neoadjuvant 1 [oxaliplatin–5-fluorouracil (5-FU)]
CRC2	CT palliative 1 (oxaliplatin–egafur uracil–bevacizumab), CT 2 palliative (UFT-irinotecan-bevacizumab)
CRC3	Untreated
CRC4	Untreated
CRC5	Untreated
CRC6	Untreated
CRC7	Untreated
CRC8	Untreated
CRC9	Untreated
CRC10	Untreated
CRC11	Untreated
CRC12	Untreated
CRC13	Untreated
CRC14	Untreated
CRC15	Untreated
CRC16	Untreated
CRC17	CT 1 palliative (5-FU oxaliplatin)
CRC18	CT 1 palliative (5-FU irinotecan)
CRC19	CT 1 palliative (5-FU), CT 2 palliative (5-FU avastin oxaliplatin), CT 3 (5-FU avastin)
CRC20	CT 1 palliative (5-FU irinotecan), CT 2 palliative (5-FU irinotecan avastin), CT 3 palliative (5-FU avastin oxaliplatin), CT 4 palliative (5-FU avastin)
CRC21	CT 1 palliative (5-FU irinotecan avastin)
CRC22	CT 1 palliative (5-FU irinotecan), CT 2 palliative (5-FU oxaliplatin), CT 3 palliative (5-FU irinotecan avastin), CT 4 palliative (5-FU avastin)
CRC23	CT 1 palliative (irinotecan 5-FU avastin), RT 1 neoadjuvant, CT 2 palliative (5-FU avastin)
CRC24	Untreated
CRC25	Untreated
CRC26	RT 1 neoadjuvant, CT 1 neoadjuvant (5-FU oxaliplatin), CT 2 neoadjuvant (5-FU irinotecan avastin), CT 3 palliative (irinotecan avastin)
CRC27	CT 1 neoadjuvant (5-FU oxaliplatin irinotecan), RT 1 neoadjuvant
CRC28	CT 1 (Camptothecin-Erbitux)
CRC29	RT 1 neoadjuvant, CT 1 neoadjuvant
CRC30	CT 1 palliative
CRC31	CT 1 palliative
CRC32	CT 1 palliative
CRC33	Untreated
CRC34	Untreated
CRC35	Untreated
CRC36	Untreated
CRC37	Untreated
CRC38	Untreated

RT, radiotherapy; CT, chemotherapy; the number indicates the sequence of treatment.

**Table W2.** Characteristics of the Selected Primers and of the Amplicons Obtained.

Species	Gene	Primer Name	Direction	Sequence 5'-3'	T <sub>m</sub> (°C)	Amplicon Size (bp)		
Human	<i>KRAS</i>	KRAS Hf 2	Sense	AATCCGTGTGGGTCAGAGAG	59.4	189		
		KRAS Hr 2	Antisense	GAAACAATAGCCACCCTCCTT	57.9	–		
Mouse	<i>KRAS</i>	KRAS Mf 3	Sense	GGCCAGGAGTGCATTAAGAC	59.4	214		
		KRAS Mr 3	Antisense	GCACGTGAGATAGTCTCCAAA	57.9	–		
Human	<i>KRAS</i>	KRAS G12V f	Sense	ACTTGTGGTAGTTGGAGCTGT	59.3	142		
		KRAS G12V r	Antisense	GAATGGTCTGCACCAGTAA	58.6	–		
Human	<i>BRAF</i>	BRAF V600E f	Sense	GATTTTGGTCTAGCTACAGA	49.7	145		
		BRAF V600E r	Antisense	TAGTAACTCAGCAGCATCTCAGG	58.8	–		
Human	<i>KRAS</i>	Kras 46 Hr	Antisense	GCTGTATCGTCAAGGCACCTC	59.4	46		
		Kras 82 Hr	Antisense	TTGGATCATATTCGTCCACAA	54.0	82		
		Kras 138 Hr	Antisense	CAAAGAATGGTCCCTGCACC	56.7	138		
		Kras 200 Hr	Antisense	TGAAAAATGGTCAGAGAAACCTT	54.7	200		
		Kras 250 Hr	Antisense	TGAAACCAAGGTACATTTCAG	56.5	250		
		Kras 300 Hr	Antisense	GAACATCATGGACCCTGACA	57.3	300		
		Kras 350 Hr	Antisense	TTCTACCCTCTCAGGAAACTCTG	60.6	350		
		Kras 400 Hr	Antisense	AAAGATTGTCTTTTAGGTCCAGATAGG	60.4	390		
		KrasNonMutated HF	Sense	GTAGTTGGAGCTGGTGGC	58.2	–		
		Kras G13D Hf	Sense	GTAGTTGGAGCTGGTGA	52.8	–		
		Kras G12V Hf	Sense	TTGTGGTAGTTGGAGCTGT	54.5	–		
		Kras G12D Hf	Sense	TGTGGTAGTTGGAGCTGA	53.7	–		
		Kras G12S Hf	Sense	ACTTGTGGTAGTTGGAGCTA	55.3	–		
		Kras G12A Hf	Sense	TGTGGTAGTTGGAGCTGC	56.0	–		
		Human	<i>BRAF</i>	Braf A1 conv k	Sense	TTATTGACTCTAAGAGGAAAGATGAA	56.9	105
				Braf A2 conv k	Antisense	GAGCAAGCATTATGAAGAGTTTAGG	59.7	–
				Braf V600E conv k	Sense	GATTTTGGTCTAGCTACAGA	53.2	97
				Braf B2 conv k	Antisense	TAGCCTCAATTCTACCATCCACA	59.3	–
				Braf blocker	Sense	GCTACAGTGAAAATCTCGATGG-PHO	–	–
				Human	<i>KRAS</i>	Kras A1 inv k	Sense	GCCTGCTGAAAATGACTGA
Kras G12D Inv k	Antisense	CTCTTGCCTACGCCAT	51.7			–		
Kras G12A Inv k	Antisense	CTCTTGCCTACGCCAG	54.3			–		
Kras G12S Inv k	Antisense	TCTTGCCTACGCCACT	51.7			60		
Kras G12C Inv k	Antisense	TCTTGCCTACGCCACA	51.7			–		
Kras G13D Inv k	Antisense	GCACTCTTGCCTACGT	51.7			64		
Kras G12V Inv k	Antisense	CTCTTGCCTACGCCAA	51.7			61		
Kras B1 inv k	Sense	CCTTGGGTTTCAAGTTATATG	54.0			67		
Kras B2 inv k	Antisense	CCCTGACATACTCCCAAGGA	59.4			–		
Kras blocker	Antisense	GCCTACGCCACCAGCTC-PHO	–			–		

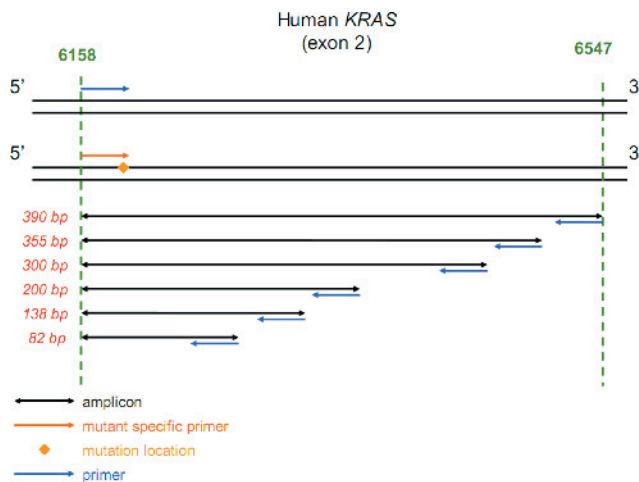


**Figure W1.** Design of the primers used for the ccfDNA size distribution study.

**Table W3.** Numerical Values of ccfDNA Quantification Obtained in the Xenografted Mice Experiments.

Mouse No.	mWT	hWT	hKRASm	hBRAFm	Tumor Weight (mg)
1	6.336	ND	ND	ND	0
2	6.627	ND	ND	ND	0
3	13.079	0.056	ND	ND	0
4	4.551	ND	0.066	ND	72.4
5	11.802	1.381	4.068	ND	89.8
6	8.29	3.644	4.304	0.201	174.8
7	3.746	2.516	1.729	ND	311.1
8	9.224	2.608	2.409	ND	358
9	6.776	1.586	6.102	0.131	465
10	5.826	8.456	7.493	0.155	543
11	9.047	9.047	12.531	0.235	1200

Data are expressed as ng/ml plasma.  
ND, not determined.

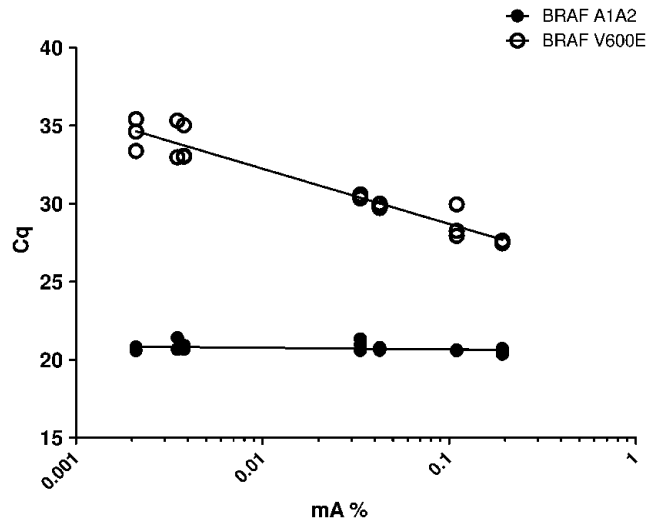


**Figure W2.** Analysis of the sensitivity of the method for detecting BRAF V600E point mutation. mA% represents the estimated mutation load and Cq represents the quantification cycle when the amplified amplicon is detected during the Q-PCR experiment. Each point corresponds to a specific amplification of the targeted sequence as determined by melting analysis. DNA from HT29 cells harboring a specific mutation was serially diluted six times into high concentrated WT genomic DNA from human placenta up to dilution of 0.2 mutated copies in 20,000 copies (1/100,000 ratio). Assay is carried in triplicate determination.